Field Dependence of Chemically Induced Dynamic Nuclear Polarization (CIDNP) in the Photoreaction of *N*-Acetyl Histidine with 2,2′-Dipyridyl in Aqueous Solution

Stefan Grosse,[†] Alexandra V. Yurkovskaya,[‡] Jakob Lopez,[§] and Hans-Martin Vieth*,[†]

Institut für Experimentalphysik, Freie Universität Berlin, Arnimallee 14, D-14195 Berlin, Germany, International Tomography Center, 630090, Institutskaya 3a, Novosibirsk, Russia, and Physical and Theoretical Chemistry Laboratory, Oxford University, South Parks Road, Oxford OX1 3QZ, U.K.

Received: December 31, 2000; In Final Form: April 3, 2001

Chemically induced dynamic nuclear polarization (CIDNP) effects for the amino acid-dye (histidine-dipyridyl) photoreaction system are measured in the range between 0 and 7 T using a novel mechanical field cycling unit with fast digital positioning of a high-resolution NMR probe in a spatially varying magnetic field. ^{1}H CIDNP effects are observed for the CH_2 protons in β-position and for two protons (H-2 and H-4) at the imidazole ring. For the protons in β-position a multiplet effect is observed having a polarization pattern that changes with the magnetic field. By analysis of the spin nutation, the non-Boltzmann population differences among the nuclear levels are determined. At a field below 20 mT "zero-field character" of the multiplet effect prevails corresponding to preferentially populated states with symmetric spin wave functions. Likewise, for the two histidine ring-protons strong polarization with an emission/absorption multiplet pattern is found between 20 and 300 mT changing below 20 mT to zero-field character. Superimposed is emissive CIDNP (net effect) for both protons. Above 0.1 T, the ring proton net effect turns absorptive and around 7 T the polarization exhibits its maximum. Numerical simulations of the field dependence in high field approximation are in very good agreement with the experimental data obtained at fields ranging from 0.1 to 7 T. The influence of different dynamic processes on the CIDNP formation and its field dependence is analyzed. Optimization of the magnetic field strength for CIDNP application in studies of protein structure and folding process is discussed.

Introduction

Chemically induced dynamic nuclear polarization (CIDNP) has for many years been successfully applied to investigating the mechanisms and kinetics of radical reactions in solution.[1,2] Important applications were the utilization of CIDNP to studying the structure of proteins[3−6] and, recently, the process of protein folding.[7] In such experiments, CIDNP effects arise in the reversible reaction between a photoexcited dye (usually a flavin) and amino acid residues exposed to the solvent. It was found that among the 20 common amino acids nuclear polarization is formed efficiently only for histidine, tyrosine, and tryptophan.[6] A systematic search was performed to find optimum conditions for the formation of nuclear polarization.[8−10] Among the adjusted parameters were the structure of the dye, the wavelength and time of light irradiation, the concentration of dye and denaturant, the temperature, and pH. Utilizing the magnetic field dependence of CIDNP effects is an effective way to increase the selectivity and sensitivity of the CIDNP method in its application to the study of proteins. Since for reasons of spectral resolution and detection sensitivity measurements are performed using NMR spectrometers working at a high field B_0 that is kept fixed, CIDNP experiments relying on variation of the external magnetic field strength are not feasible with standard equipment. For solving this problem, the concept of employing the stray field of the NMR magnet for polarization followed by a fast transfer of the sample to the NMR detection coil using a flow system with a pneumatically driven syringe has been applied.[10,11] In this way, it was possible to measure CIDNP effects in a magnetic field range from about 0.1 to 7 T.

From experience with other radical pair reactions, it is known that commonly the conditions for CIDNP formation are more favorable when going to an even lower polarization field comparable with the local hyperfine interactions ($B_{pol} \cong |A|$).[1,2] At such a low field the singlet state (S) and all three triplet sublevels (T_+, T_0, and T_-) of the radical pair are effectively involved in the spin evolution, while at high magnetic field only the $S-T_0$ transitions prevail. Hence, for comparative studies of CIDNP formation it is important that they are done in a field range from 0 to several Tesla, while all other parameters are kept fixed. For covering this whole range, we used a different experimental approach for cycling the field employing modern digital positioning techniques. Our concept is based on varying the field by precise positioning of the NMR probe in the stray field along the symmetry axis of the cryomagnet of the spectrometer. There the photoreaction is run and CIDNP formed. Subsequently, the whole probe is quickly transferred to the center of the magnet, where the NMR spectra are recorded. As an option, the polarization field can be varied from 0 to 0.1 T by setting the current of an electromagnet located under the cryomagnet. Another advantage of this approach distinguishing it from alternative field cycling methods is the feasibility of sample rotation and thus of keeping high spectral resolution, which is a prerequisite for the analysis of individual NMR

* Address all correspondence to Prof. Dr. H.-M. Vieth, Freie Universität Berlin, Institut für Experimentalphysik, Arnimallee 14, D-14195 Berlin, Germany, Telephone: +49-30-838 55062, Fax: +49-30-838 56081, E-mail: Hans-Martin.Vieth@physik.fu-berlin.de.

[†] Freie Universität Berlin.

[‡] International Tomography Center.

[§] Oxford University.

10.1021/jp004582i CCC: $20.00
Published on Web 06/07/2001

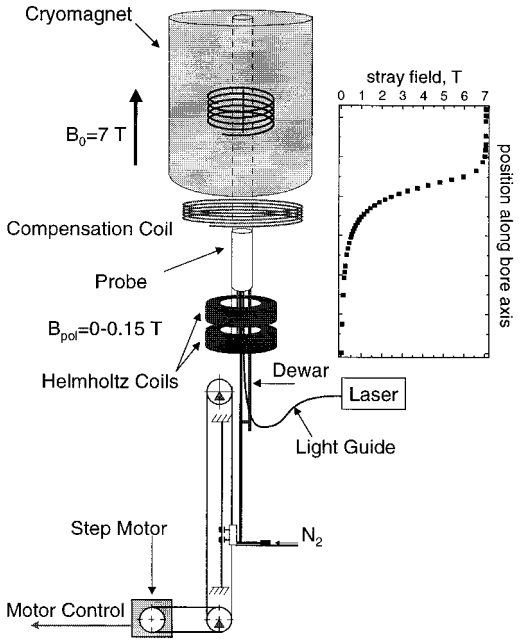

Figure 1. Field cycling setup with mechanical probe transfer. Inset shows magnetic field amplitude as function of position along the transfer path.

transitions. The design of the setup is briefly described in the Experimental Section, and a more detailed description is presented in ref 12.

Previous work has shown that 2,2′-dipyridyl is an efficient dye for CIDNP in protein and amino acids.[8] Its photoreaction with the *N*-acetyl derivatives of tryptophan,[13] tyrosine,[14] and histidine[15] was in its main steps established by using time-resolved CIDNP (tr-CIDNP) at high magnetic field ($B_0 = 7$ T) and laser flash photolysis. Focus of our study is the comparative analysis of high and low field CIDNP, since it allows one to characterize the mechanisms of the CIDNP formation and to extract dynamic and structural data about reaction intermediates. In this paper, we study the CIDNP field dependence under stationary irradiation (cw-CIDNP) for *N*-acetyl histidine in the reaction with 2,2′-dipyridyl in aqueous solution with particular attention paid to the magnetic field range below 0.1 T and to the differences in polarization pattern for the individual atomic positions in the amino acid. A comparative study of tyrosine and tryptophan, which will allow fine adjustment of experimental conditions for protein investigation, is under way in our laboratory, and the results will be published later.

Experimental Section

Mechanical field cycling was set up allowing field variation between earth magnetic field and 7 T with high-resolution NMR detection under slow sample rotation. The layout is shown in Figure 1. Employing a step-motor driven transfer along the bore axis of the 7 T cryomagnet, the whole NMR probe moves inside the bearing tube with an accuracy and reproducibility better than 0.1 mm between the center of the cryomagnet coil and any position along the bore axis. Maximum shuttling distance is 620 mm matching the center of an electromagnet (Helmholtz pair) placed below the cryomagnet vessel. The shortest transfer-time of the NMR probe is 0.3 s for the full distance; for other positions, it is shorter. Since the setup allows stopping the probe at every desired position along the transfer path, it is possible to utilize the gradient of the stray field of the cryomagnet and thus to measure photo-CIDNP in the full field range up to 7 T.

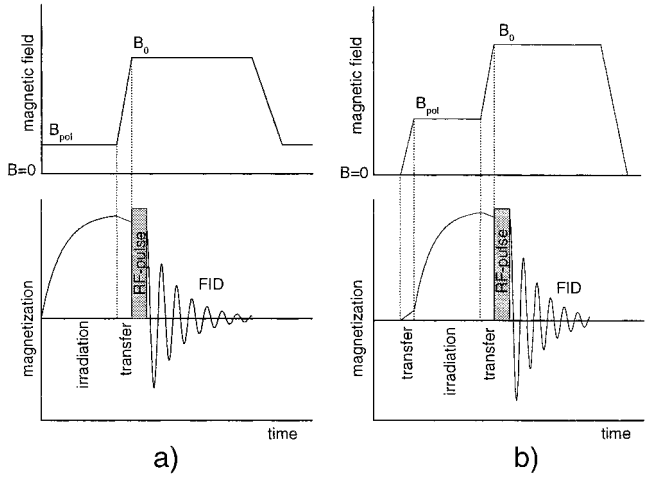

Figure 2. Timing schemes of CIDNP experiments with field cycling. (a) polarization in field of electromagnet, 0.05 mT < B_{pol} < 0.12 T, (b) polarization in stray field of cryomagnet, 0.1 T < B_{pol} < 7 T. Typical times: light irradiation time $t_L = 0.1-30$ s; transfer time $\Delta t = 0.3-2$ s; rf pulse duration $1-60$ μs.

Field resolution is limited by the field variance in the relevant sample volume, which is determined by the geometric profile of the light beam. At the maximum field gradient of about 70 T/m at around 5 T (see Figure 1 for the contour of the gradient) the resolution is thus 350 mT with a step size of 5 mT. At fields below 0.1 T where sharp CIDNP features are likely, which require much higher resolution, field variation is achieved by control of the electric current through the Helmholtz coils allowing a resolution better than 0.05 mT and minimum step size of 0.1 mT.

Light is irradiated onto the sample by a XeCl excimer laser through a flexible liquid light guide with a 90° prism on the top. This design provides for constant irradiation conditions across the full field range. The laser operates at 308 nm wavelength, 50−200 Hz repetition frequency, and about 4 mJ/pulse output power. Each experiment starts with irradiating light for a certain time t_L onto the sample at a preselected magnetic field B_{pol}. Directly after stopping light irradiation, the sample is transported within a time Δt to the center of the cryo-coil (observation field $B_0 = 7$ T), where NMR detection is performed immediately. The full timing scheme is shown in Figure 2, where the left part refers to measurements with the electromagnet, while the right part applies to positioning in the stray field of the cryomagnet. To estimate effects of relaxation on the CIDNP intensities, we made test measurements at zero and at high polarization field with an extra waiting time of variable duration before transfer to observation field. By stepwise increase of this waiting time, we mapped out the polarization decay to thermal equilibrium. The shortest time constant is observed at zero field with about 4 s for the histidine ring and β-CH_2 protons. Accordingly, with our settings of $t_L = 2$ s and $\Delta t = 0.5$ s the loss in polarization is kept below 30%.

Since the field change occurs adiabatically, the population of the individual nuclear spin eigenstates is conserved. Usually the whole cycle is repeated again, but without light irradiation, and the two NMR acquisitions are subtracted from each other to get rid of background signal due to unavoidable thermal polarization. By stepwise variation of B_{pol}, the field dependent polarization for all nuclear positions is mapped out.

The sample containing 0.5 mL of solution was purged with pure nitrogen gas and sealed in a standard 5 mm Pyrex NMR tube. The tube fits into a ceramic spinner system for slow sample rotation (0−150 Hz) integrated into the NMR probe. The rotor

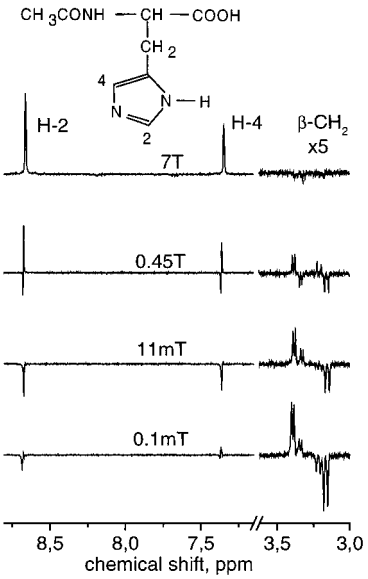

Figure 3. ^{1}H CIDNP spectra of histidine, at different polarization field B_{pol} showing change in polarization pattern. All spectra recorded after $\pi/4$ rf excitation pulse; only polarized lines are shown.

SCHEME 1

$$DP + h\nu \rightarrow {}^{T}DP \quad (1)$$

$${}^{T}DP + HisH_2^{+} \rightarrow {}^{T}(DPH\cdot + HisH^{+}\cdot) \quad (2)$$

$${}^{T}(DPH\cdot + HisH^{+}\cdot) \leftrightarrow {}^{S}(DPH\cdot + HisH^{+}\cdot) \quad (3)$$

$${}^{S}(DPH\cdot + HisH^{+}\cdot) \rightarrow DP + HisH_2^{+} \quad (4)$$

runs continuously keeping sufficient stability during the whole cycle. To prevent vortex formation and sample shaking during the transfer, a Teflon plug is inserted into the tube on the top of the liquid.

Chemicals. D_2O (Aldrich), 2,2′-dipyridyl (Aldrich), and *N*-acetyl histidine (Sigma) were used as received.

Results and Discussion

Reaction Scheme. In previous work, it was established that the reaction between dipyridyl and *N*-acetyl histidine (see Figure 3 for the structures) strongly depends on pH.[15] This fact was attributed to the dependence of the concentration of reactive species on the pH of aqueous solutions. The imidazole ring of *N*-acetyl histidine can be in positively charged ($HisH_2^+$, pK_a = 6.1), in neutral (HisH, pK_a = 14.5), or in negatively charged deprotonated form (His^-).[16] Dipyridyl can exist either in protonated (DPH^+, pK_a = 4.3)[17] or in neutral (DP) state. No reaction takes place between protonated dipyridyl (DPH^+) and protonated histidine ($HisH_2^+$), the situation met at pH < 3. In the range 4 < pH < 8 the quenching of dipyridyl in its excited triplet state ^{3}DP by protonated histidine ($HisH_2^+$) proceeds via hydrogen atom transfer with rate constant[15] $k_H = 1.2 \times 10^8$ M^{-1} s^{-1} (Scheme 1).

The observed reaction rate constant k_q^{obs}, which describes the dependence of the triplet decay rate on the total concentration of *N*-acetyl histidine in the solution, has its maximum at pH = 6.0. All experiments were taken at pH = 5.6, at a histidine concentration of 0.02 M chosen to ensure that all ^{T}DP triplets are efficiently quenched by histidine, while the concentration of DP was set to 2×10^{-3} M to yield an optical density of 0.7 at 308 nm for the 4-mm optical pathway inside the NMR sample tube.

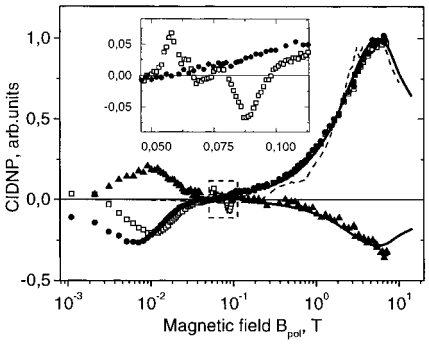

Figure 4. CIDNP net effect as function of polarization field B_{pol}, for H-2 (●) and H-4 (□) protons and β-CH_2 (▲). Dashed (- - -) and solid line (—) simulations (see text).

CIDNP Spectra. The cw-CIDNP spectrum obtained at B_{pol} = 7 T (Figure 3, top trace) is in good agreement with the results obtained by time-resolved CIDNP techniques, where the NMR signal is recorded after a single laser flash and the time evolution is mapped out by varying the delay between laser and rf detection pulses.[15] The main difference of the spectra obtained under cw-irradiation (present work and ref 12) with respect to time-resolved experiments concerns the relative intensities of the lines: in cw-CIDNP the emissive signals of dipyridyl and of the histidine β-CH_2 protons are much weaker than the absorption lines of the H-2 and H-4 protons. While the signs of CIDNP effects for the histidine protons at this field match those obtained by tr-CIDNP, the corresponding stationary amplitudes do not agree, and the causes for that will be discussed later. We attribute the relatively small CIDNP amplitude of the dipyridyl signals in the cw-experiments to the low dye concentration. At our experimental conditions, the number of absorbed photons during light irradiation is much larger than the number of dye molecules in the irradiated volume; therefore, each of these molecules participates in several photoreaction cycles, and this circumstance limits the accumulation of CIDNP for DP in the sample.

Spectra obtained at different magnetic fields (0.1 mT, 11 mT, 0.45 T, and 7 T), but otherwise identical experimental conditions are shown in Figure 3. The spectral patterns change substantially with variation of the magnetic field strength. Two new features are observed at low magnetic field with respect to the CIDNP at 7 T. The first feature is the splitting of each of the two singlet lines of the ring protons H-2 and H-4 into two components with opposite sign of polarization. This is typical for the so-called "multiplet effect" of CIDNP that manifests itself as antisymmetric enhancement with respect to the center of the multiplet: one-half of the multiplet lines is in emission (E) and the other part is in absorption (A). This multiplet effect is superimposed on net absorptive or net emissive polarization depending on the magnetic field strength. Second, for the β-CH_2 protons strong multiplet polarization is detected with increasing amplitude toward a magnetic field of 10 mT and below.

Field Dependence of CIDNP Net Effect. In Figure 4 the net effect, i.e., the integrated polarization of the respective NMR multiplet, for the H-2 and H-4 protons is shown as a function of polarizing field B_{pol} on logarithmic scale. The highest emissive polarization is found near the low field end of the CIDNP curve, with the maximum for H-2 at about 7 mT and for H-4 at 11 mT. At a field of about 70−90 mT, the sign of net CIDNP changes. In this region, a few small sharp peaks of different sign are visible in the field dependence of the H-4 proton (see Figure 4, inset). Similar features but less pronounced are found also for the H-2 proton near 40 mT. At higher

magnetic field, the field dependencies for H-2 and H-4 coincide within the experimental accuracy, and both signals grow with increase of the magnetic field up to about 7 T. The CIDNP field dependence of the β-CH_2 protons, which is included in Figure 4, looks almost like a mirror image of that for the ring protons, with opposite sign and reduced amplitude.

Information about radical pair properties, which can be extracted from cw-CIDNP experimental data, lies in the sign of the effects and in the position of the extrema on the field scale. Singlet−triplet transitions in the radical pair (reaction step 3 in Scheme 1) are crucial for CIDNP formation, and the contribution from individual triplet electronic substates depends on the magnetic field strength. At low external field, the radical pair singlet state is coupled with all three triplet states mainly due to hyperfine interaction (HFI) with magnetic nuclei in the radical pair, while at high field both, the difference of electronic *g*-factors of the radical pair partners and HFI are important for singlet−triplet spin evolution. At high magnetic field only $S-T_0$ transitions are important, which depend in their efficiency on the nuclear spin orientation and thus cause a spin-sorting, while at low magnetic field CIDNP effects arise as the result of competition between $S-T_-$ and $S-T_+$ transitions, which are accompanied by opposite nuclear spin flips. Analysis of multiplet and net effect at variable magnetic field provides information, which is not available from high field CIDNP experiments.

Calculation of Net CIDNP. To check the importance of the individual polarization channels and to see what level of sophistication is necessary for a quantitative simulation of the experimental data and a reliable evaluation of the magnetic parameters, we analyzed net and multiplet CIDNP as function of B_{pol}. For numerical simulation of the CIDNP field dependence, we followed the model suggested by Adrian.[18] To curb the computational effort, he makes use of a high-field approximation (taking only $S-T_0$ transitions into account). The radical pair is described by the magnetic Hamiltonian:

$$\hat{H}^{(M)} = \beta_0(g_1\hat{S}_1 + g_2\hat{S}_2)B_{pol} + \sum_{n=1}^{N_1} A_{1n}\hat{I}^n_{1z}\hat{S}_{1z} + \sum_{m=1}^{N_2} A_{2m}\hat{I}^m_{2z}\hat{S}_{2z} \quad (5)$$

Here, β_0 is the Bohr magneton, B_{pol} is the external magnetic field strength, g_1 and g_2 are the electronic *g*-factors of radicals 1 and 2, A_{1n} and $\hat{I}^n_{1z}$ are, respectively, the isotropic hyperfine structure constant and the nuclear spin operator acting on the *n*th nucleus of radical 1, and A_{2m} and $\hat{I}^m_{2z}$ are the analogous quantities for radical 2. N_1 and N_2 are the numbers of nuclei, $\hat{S}_{1z}$ and $\hat{S}_{2z}$ are the S_z electron spin operators of radical 1 and 2, respectively. The transition matrix element between singlet S and triplet T_0 states of the radical pair is in perturbation theory given by the following expression:

$$H^{(M)}_{ab} = \frac{1}{2}\beta_0 B_{pol}(g_1 - g_2) + \frac{1}{2}\sum_{n=1}^{N_1} A_{1n}M_{1n}{}^{(a)} - \frac{1}{2}\sum_{m=1}^{N_2} A_{2m}M_{2m}{}^{(b)} \quad (6)$$

Here, the subscript *ab* denotes a particular nuclear spin configuration with the total magnetic quantum number *M*, $M_{1n}{}^{(a)}$ being the magnetic quantum number of the *n*th nucleus of radical 1 in the overall nuclear spin state *a*, $M_{2m}{}^{(b)}$ the magnetic quantum number of the *m*th nucleus of radical 2 in the overall nuclear spin state *b*.

SCHEME 2: Structure and Hyperfine Couplings (in mT) of the Radical Partners (for details see text)

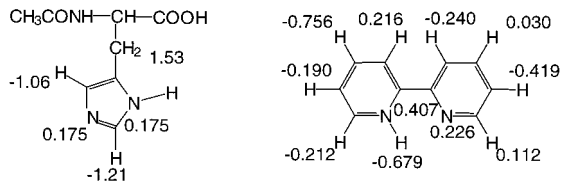

Under the assumption that the singlet character of the radical pair wave function makes only small changes during the time of the radical diffusive displacement (τ is the meantime between diffusive replacement):[1,18]

$$(|H^{(M)}_{ab}|\tau)^{1/2} \ll 1 \quad (7)$$

the chemically induced difference in population *N* between two nuclear spin states (*ab*) and (*a′b′*) of a recombination product formed out of the radical pair singlet state is given by the relation:

$$N_{ab} - N_{a'b'} = P_0[(|H^{(M)}_{ab}|)^{1/2} - (|H^{(M)}_{a'b'}|)^{1/2}] \quad (8)$$

P_0 is a normalization constant. In the calculation for a radical pair with several ($N = N_1 + N_2$) nuclei, expression 6 has to be summed over all nuclear spin configurations of both radicals. The CIDNP field dependencies of H-2, H-4, and β-CH_2 protons were calculated according to eq 8 for the magnetic field range from 0.01 to 10 T. In the calculation, we used $g_1 = 2.00226$ for the histidine cation radical, which is of π-type,[19] and negative isotropic hyperfine coupling constants for the protons at the histidine imidazole ring, ($A_{H-2} = -1.21$ mT, $A_{H-4} = -1.06$ mT).[19] The corresponding data on HFI for the β-CH_2 protons are unavailable (cf. ref 20). However, the isotropic part of HFI for these protons is related via hyperconjugation to the π-spin density at the neighboring C-atom and usually is positive.[21] As an estimate for HFI, we used data taken from the 2-methylimidazole radical, for β-CH_2 the value of 1.53 mT for the methyl protons and 0.175 mT for both nitrogen atoms.[19] For the dipyridyl radical $DPH^{\bullet}$, we are not aware of corresponding experimental data; therefore, a set of calculated isotropic hyperfine constants[22] (as shown in Scheme 2, in mT) and $g_2 = 2.00300$ obtained for the anion radical[23,24] was used.

The results of these calculations for the different protons of histidine are included in Figure 4 (solid lines). The agreement of the calculated curve with the experimental data is very good for both ring protons and still reasonably good for the β-CH_2 protons, despite the rather simplified theoretical approach used in the simulation of CIDNP. However, the good accordance with experimental data is restricted to fields around 0.1 T and above, showing the lower limit for application of the high-field approximation.

Important for the quantitative agreement was that all hyperfine couplings were taken into account. For demonstration, the analogous calculation, but considering only the hyperfine interaction of magnetic nuclei in the histidine radical and none of the dipyridyl protons, is shown by the dashed line. In this case, the maximum is slightly shifted to lower field and a few peaks of small amplitude are seen superimposed upon the smooth curve. The peaks on the curve appear at positions where terms $H^{(M)}_{ab}$ change sign. The amplitude of these structures reduces when more nuclei are taken into account and vice versa. If the calculation is restricted to only one nucleus with $A_i \approx 1$ mT and $\Delta g = 2.00300 - 2.00226 = 7.4 \times 10^{-4}$, the field

dependence becomes a sharp, spike-like structure with its maximum at $B_{pol}^{max} = 740$ mT (not shown).

Careful measurements allowed us to resolve several sharp features showing up in the CIDNP field dependence of the H-4 proton in the range between 0.05 and 0.1 T (see Figure 4, inset). The field dependence for β-protons and H-2 shows similar but less pronounced structures in this region. We assume that these features correspond to conditions of the type $H_{ab}^{(M)} = 0$. To verify this assumption, comparative CIDNP experiments employing deuterated dipyridyl with its reduced HFI are planned.

Low Field CIDNP Analysis. At low magnetic fields, when the first term in eq 6 becomes negligible, the hyperfine coupling elements are crucial for singlet triplet transitions. Since the isotropic HFI constants of the H-2 and H-4 protons in the histidine radical cation are reported to be very similar (−1.06 and −1.21 mT for H-2 and H-4, respectively), one expects that the CIDNP field dependencies for these protons coincide not only at high magnetic field, but in particular in the low field regime. The remarkable difference of 4 mT between the CIDNP maximum position of H-2 and H-4 protons (see Figure 4) could thus serve as a hint that the histidine radical participating in our photoreaction has a structure with largely differing HFI constants. This would confirm recent results described by Lassmann et al.,[20] who discussed the electronic structure of the transient histidine-OH adduct radical formed in aqueous solution by oxidation of histidine with Ti^{3+}/H_2O_2 and assigned a large hyperfine constant of 3.02 mT to the H-4 proton and one of 0.59 mT to the H-2 proton. However, having such a strong difference of hyperfine constants these two protons would exhibit differences in their CIDNP characteristics clearly at high magnetic field, in contrast to our results (see Figure 4). That is why we believe that such an explanation is not applicable, and the presence of any σ-radical of histidine in the photoreaction with 2,2′-dipyridyl in solution is highly unlikely.

Different positions of maximum in net CIDNP at low field can, in principle, be caused by a contribution of the $S-T_{\pm}$ mechanism of CIDNP formation, if one assumes strong influence of the electronic exchange interaction. The emissive sign of the net signal taken together with triplet multiplicity of the radical pair would then point to a negative exchange integral, because in frame of the $S-T_{\pm}$ mechanism the sign Γ of nuclear polarization is determined by the sign of the product of precursor multiplicity μ (μ is equal to +1 for triplet and −1 for singlet precursor) and that of exchange integral J:

$$\Gamma = \mu J \tag{9}$$

Expression 9 is applicable in the case that the magnitude of 4J is larger than the magnitude of the HFI constant.[1] This is not impossible for the π-type cation radical of histidine. Also, the argument that for the $S-T_{-}$ mechanism the field position of the emissive maximum is given by the value of the exchange interaction, hence has to be identical for all nuclei, and is in contradiction to our results showing different positions is not convincing. Considering that the H-2 and H-4 lines form one common multiplet (so-called AX nuclear spin system), they have to be taken together. Integration over the multiplet composed of the H-2 and H-4 lines shows net emission with its maximum at nearly the same magnetic field as for the β-CH_2-protons. A stronger argument against significant contribution by the $S-T_{-}$ CIDNP channel is the observed pronounced multiplet effect, which cannot be formed by $S-T_{-}$ transitions, because such a spin-flip mechanism would lead to net emission only. For the same reason, the $S-T_{-}$ mechanism fails to explain the absorptive sign of net polarization for the β-CH_2-protons observed at the same magnetic field range. Theory predicts for $|J| > |A|/4$ that the $S-T_{-}$ mechanism leads only to emissive CIDNP independent of the sign of the HFI constant.[1] Therefore, the different sign of polarization unambiguously rules out that the $S-T_{-}$ mechanism with an average exchange integral (−2 J) of about 9 mT is responsible for the observed CIDNP.

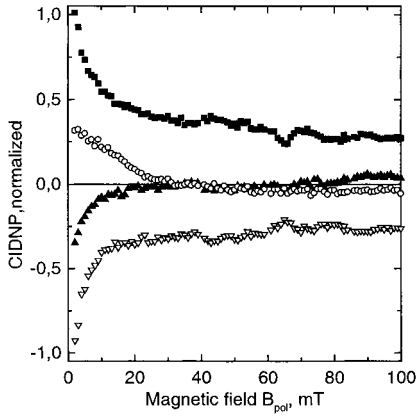

Figure 5. CIDNP of individual lines of β-CH_2 proton multiplet as function of polarization field B_{pol} (▽, β_1; ▲, β_2; ○, β_3; ■, β_4). $\pi/4$ rf detection pulse. Line assignment as shown in Figure 6.

All these considerations show that neither the proposed σ-radical structure of histidine in the reaction with 2,2′-dipyridyl nor the $S-T_{\pm}$ mechanism of CIDNP can give a self-consistent explanation of our data. Therefore, the low field polarization behavior requires a more detailed discussion of CIDNP *net* and *multiplet* effect of all protons.

Multiplet Effect of CIDNP. Figure 5 shows the CIDNP field dependencies for the set of lines related to the β-CH_2 positions. Two qualitatively different multiplet patterns can be distinguished. In Figure 3, the striking difference of CIDNP at $B_{pol} = 0.1$ mT and $B_{pol} = 450$ mT is obvious.

In the upper field range of about 0.2−4 T, the multiplet effect observed is characterized by an alternating sign of polarization (A/E − A/E) with equal intensity of all four components of the β-CH_2 signal (the additional finer splitting of each component into two lines is neglected) and an E/A pattern for each, H-4 and H-2, signal. (Type A/E means absorption at low field and emission at high field part of a multiplet).

The spin−spin coupling between the H-2 and H-4 protons is only $J = 1.54$ Hz. This value is below the resolution of the experimental spectra obtained by field cycling with the result that the components of the corresponding CIDNP doublet are strongly overlapping (the width of individual lines is about 3 Hz). Thus, the observed multiplet CIDNP effect corresponds to what is left from two overlapping lines of opposite sign. For the ring protons, therefore, the experimental data are not suited for quantitative analysis.

In contrast, the β-CH_2 signals are well resolved, and hence net and multiplet effect of CIDNP can be separated and analyzed quantitatively. The protons in the β-CH_2 group are nonequivalent in the diamagnetic molecule; hence, the ^{1}H NMR signals form a quartet characteristic for an AB system with the two inner lines having higher intensity. Because of further nuclear spin−spin interaction with the proton in α-CH-position, each of these four lines in the quartet is split into two lines of equal intensity with the result that the signals from the protons form an octuplet as is characteristic for an ABM structure. The proton in α-CH-position itself does not exhibit CIDNP; therefore, the analysis can be done using a Hamiltonian of the diamagnetic molecule reduced to an AB spin system of two β-CH_2 protons only, and

the spin−spin interaction with the α-CH proton can be neglected as far as formation of polarization is concerned. Analysis goes according to the Kaptein rules for multiplet effect:[24]

$$\Gamma_{ij} = \mu\epsilon A_i A_j J_{ij} \sigma_{ij} \tag{10}$$

where the sign of Γ_{ij} stands for the type of multiplet effect, E/A for positive and A/E for negative Γ_{ij}, respectively. Here the values $\mu = 1$ and $\mu = -1$ correspond to triplet and singlet precursor multiplicity, respectively, $\epsilon = 1$ to geminate products, $\epsilon = -1$ to products from escaped radicals, A_i, A_j represent the hyperfine coupling of protons i and j, J_{ij} the scalar coupling, $\sigma_{ij} = 1$ if both nuclei belong to the same radical and $\sigma_{ij} = -1$ if both nuclei belong to different radicals. For both cases (ring and β-CH_2 protons), $\mu = 1$, $\beta = 1$, $\sigma_{ij} = 1$, and the sign of the product (A_iA_j) is positive. For the ring protons with positive J_{ij} Γ is, therefore, positive, and accordingly an E/A type doublet is observed for both, H-2 and H-4. The coupling between the two β-CH_2 protons J_{ij} is negative, hence Γ is negative, and the sign of CIDNP multiplet effect is (A/E − A/E) in accordance with our observation. At fields above 3 T the multiplet effect is concealed by a net effect, since the difference of *g*-factors plays here the dominant role in the intersystem crossing.

A different pattern of multiplet effect is detected at low magnetic field. In the β-CH_2 multiplet, the intensity of the outer components is much stronger than the intensity of the two inner lines, the sign of the two low field lines is absorptive and of the two high field lines emissive. At a magnetic field below 20 mT, this pattern of multiplet polarization is prevailing, with the intensity of the outer components strongly increasing with the decrease of the magnetic field. For the imidazole ring multiplet, too, the line pattern is changing with the decrease of the magnetic field to a few mT. The outer components increase, while the inner lines decrease to zero. For each nuclear position, only a single line is observed, while the second component vanishes. At $B_{pol} = 0.1$ mT, these "singlets" acquire a different sign of polarization, namely, H-4 gets absorptive and H-2 becomes emissive.

This change of CIDNP pattern is in accordance with the "(n−1) multiplet effect"[26] or zero-field multiplet effect, which was first detected by Fischer and Lehnig.[27] The name "n−1" comes from the absence of one line in the CIDNP pattern of every NMR multiplet as observed in cw-NMR experiments. The origin of this phenomenon is briefly described as follows: At zero magnetic field, and when dipolar couplings are negligible, the nuclear spin Hamiltonian of the reaction product reduces to $\hat{H}^p = \sum_{i>j} J_{ij} \hat{I}_i \hat{I}_j$. With the total nuclear spin operator $\hat{K} = \sum_i \hat{I}_i$, the Hamiltonian is diagonal in K-representation, because $|\hat{H}^p, \hat{K}^2| = 0$, $|\hat{H}^p, \hat{K}_z| = 0$. Therefore, the nuclear states of the diamagnetic molecule are eigenstates of $\hat{K}^2$ and $\hat{K}_z$. They are characterized by the quantum numbers K and M_K; the nuclear spin states within the same K branch are degenerate and indistinguishable from each other at zero field. This phenomenon reflects the fact that at zero magnetic field there is no preferred external axis for the quantization of the nuclear spins. When the spin system is polarized at zero magnetic field and adiabatically transferred to high magnetic field for detection the resulting slow passage cw-NMR spectrum consists of a so-called "n−1 multiplet".

However, this description of the polarization pattern is not straightforward applicable to FT-NMR detection with nonselective rf excitation pulses. For pulsed FT-NMR spectroscopy of a coupled spin system, which is not in Boltzmann equilibrium, it is known that only in the limit of small flip angle $\varphi = \gamma B_1 \tau$ (here, γ denotes the nuclear gyromagnetic ratio, B_1 the rf magnetic field, and τ the pulse duration) the intensity of a line is proportional to the population difference ($P_i - P_j$) of the corresponding transition, but that for finite nutation the spectral intensity pattern is a function of φ.[28] The analysis of this dependence (which is considered below) allows one to extract the population difference induced by chemical reaction.

Considering an AB nuclear spin system of a diamagnetic molecule the spin-Hamiltonian (in units of h) is in high field approximation given by:

$$\hat{H} = -\nu_0(1 - \sigma_A)\hat{I}_{zA} - \sigma_0(1 - \sigma_B)\hat{I}_{zB} + J_{AB}\,\hat{I}_{zA}\,\hat{I}_{zB} \tag{11}$$

where ν_0 is the Larmor frequency of a free proton, J_{AB} is the nuclear spin−spin coupling constant, σ_A and σ_B the chemical shift of the nuclei A and B, respectively.

The corresponding eigenstates are as follows:

$$|1\rangle = |\alpha\alpha\rangle = t_+ \qquad E_1 = \nu_0(-1 + {}^1/_2\sigma_A + {}^1/_2\sigma_B) + {}^1/_4 J_{AB}$$

$$|2\rangle = \cos\theta|\alpha\beta\rangle - \sin\theta|\beta\alpha\rangle \qquad E_2 = -{}^1/_4 J_{AB} - C$$

$$|3\rangle = \sin\theta|\alpha\beta\rangle + \cos\theta|\beta\alpha\rangle \qquad E_3 = -{}^1/_4 J_{AB} + C$$

$$|4\rangle = |\beta\beta\rangle = t_- \qquad E_4 = \nu_0(1 - {}^1/_2\sigma_A - {}^1/_2\sigma_B) + {}^1/_4 J_{AB}$$

where the parameters C and θ are given by $C = {}^1/_2\sqrt{(J_{AB})^2 + \nu_0^2(\sigma_A - \sigma_B)^2}$, and $\theta = {}^1/_2 \arctan\{J_{AB}/\nu_0(\sigma_A - \sigma_B)\}$. For incoherent nonequilibrium states (also called nonequilibrium states of the first kind), as applicable to CIDNP, the line intensities for a strongly coupled two-spin $^1/_2$ system AB are described by the following four coupled equations.[28,29] Depending on the nutation angle $\varphi = \gamma B_1 \tau$, the lines of the β-CH_2 proton multiplet have the following intensities β_i:

$$\beta_1 = \frac{1}{2}\sin\varphi \times [\cos^2(\varphi/2) \times (1 - \sin 2\theta) \times (P_3 - P_1) + \sin^2(\varphi/2) \times \cos^2 2\theta \times (P_3 - P_2) + \sin^2(\varphi/2) \times (1 - \sin 2\theta) \times (P_4 - P_3)] \tag{12}$$

$$\beta_2 = \frac{1}{2}\sin\varphi \times [\cos^2(\varphi/2) \times (1 + \sin 2\theta) \times (P_2 - P_1) - \sin^2(\varphi/2) \times \cos^2 2\theta \times (P_3 - P_2) + \sin^2(\varphi/2) \times (1 + \sin 2\theta) \times (P_4 - P_2)] \tag{13}$$

$$\beta_3 = \frac{1}{2}\sin\varphi \times [\sin^2(\varphi/2) \times (1 + \sin 2\theta) \times (P_2 - P_1) + \sin^2(\varphi/2) \times \cos^2 2\theta \times (P_3 - P_2) + \cos^2(\varphi/2) \times (1 + \sin 2\theta) \times (P_4 - P_2)] \tag{14}$$

$$\beta_4 = \frac{1}{2}\sin\varphi \times [\sin^2(\varphi/2) \times (1 - \sin 2\theta) \times (P_3 - P_1) - \sin^2(\varphi/2) \times \cos^2 2\theta \times (P_3 - P_2) + \cos^2(\varphi/2) \times (1 - \sin 2\theta) \times (P_4 - P_3)] \tag{15}$$

Here, the P_i are the populations of the corresponding eigenstates. The nutation pattern obtained at 0.1 mT is presented in Figure 6. From the simulation of the nutation pattern with normalizing of signal β_4 at its maximum to unity the following values ($P_i - P_j$) of population differences are obtained: $P_2 - P_1 = P_2 - P_4 = 0.24$, $P_4 - P_3 = P_1 - P_3 = 1.54$, $P_2 - P_3 = 1.78$. These data confirm that at 0.1 mT the populations P_1, P_2, and P_4 are remarkably different from P_3. For negative J_{AB}, the

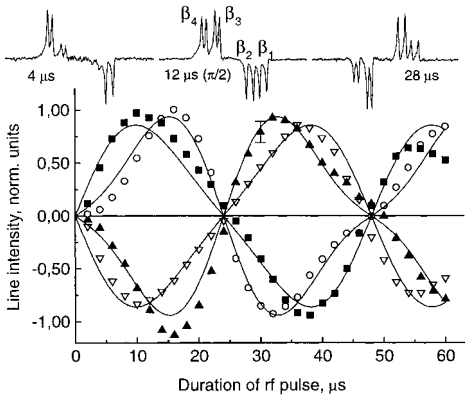

Figure 6. CIDNP nutation of β-CH_2 protons. Line assignment (∇, β_1; ▲, β_2; ○, β_3; ■, β_4) as shown in the middle spectrum inserted above the plot. Full lines represent simulations with the population numbers given in the text (parameter of relative coupling strength $\theta = -8.4°$).

states $|1\rangle$, $|2\rangle$, and $|4\rangle$ correspond to the triplet t_+, t_0, and t_- nuclear states at zero magnetic field, while state $|3\rangle$ corresponds to the singlet state *s*. Our simulation shows, that the differences of population within the triplet manifold are small. The population difference ($P_2 - P_3$) is nonobservable by a single-pulse NMR experiment, but our simulation shows that it is rather large, too. A similar analysis has been done for a magnetic field of 10 and 50 mT. As it shows the difference ($P_2 - P_3$) reduces with increasing magnetic field reflecting the transition from zero-field regime to high-field regime. For the multiplet effect at high magnetic field, the states $|2\rangle$ and $|3\rangle$ of antiparallel spin orientation are populated equally and differ from the states $|1\rangle$ and $|4\rangle$ with parallel orientation of nuclear spins.

The nutation pattern for the H-2 and H-4 protons at $B_{pol} = 50$ mT was analyzed previously,[12] and from the characteristic nutation with frequency $\omega_{nut} = 2 \times \gamma B_1$ the nature of multiplet effect was verified to be due to an AX system. The line shape of these signals at low field confirms that for the H-2 and H-4 protons, too, the polarization pattern is in accord with the discussed low field multiplet effect. Because of the lack of sufficient spectral resolution the characteristic features are slightly modified: the low field component of H-2 has a larger amplitude than the high field component and for both ring protons the low field lines are emissive; the high field component of H-4 has a larger amplitude than the low field signal, and for both protons the high field lines are absorptive. Modeling an AX system by eqs 12−15 with appropriate values of spectroscopic parameters [$J_{AX} = 1.5$ Hz and $(\Omega_X - \Omega_A) = 2\pi \times 411$ Hz] results in preferential population of the singlet state of the AX system in contrast to the population difference obtained for the β-CH_2 group.

The nonresolved zero-field type multiplet effect is for both ring protons superimposed by net emissive CIDNP, again with its maximum at a magnetic field of about 7 mT. The resulting CIDNP as the sum of both effects has, therefore, in case of the H-2 signal, where both contributions are negative, its maximum at lower magnetic field than for the signal of H-4. That the shape of the CIDNP field dependence, when we integrate over the aromatic region, coincides with the net CIDNP obtained for the β-CH_2 protons supports our interpretation.

Our data show that for the β-CH_2 protons the signals of the "zero field" pattern decrease in intensity by 50% at a magnetic field of about 5 mT and reach a saturation plateau above 15 mT. At low magnetic field the intersystem transitions occur under coherent electron spin motion induced by hyperfine interaction. The transition from "zero field" to high field spin effect is expected at about a field, when the spin quantization axis changes from the molecular frame of reference (MFR) with the local magnetic field determined mainly by the axes of the hyperfine interaction tensor to the laboratory frame of reference (LFR) with the external magnetic field B_{pol} as symmetry axis. It means that the spin motion around axes in the radical pairs with uncorrelated orientation changes to the case of parallel precession axes. The effective hyperfine field of each radical *k* is defined as $B_k^{hfc} = \sqrt{\sum_{i=1}^{N} I_i(I_i+1)A_{ik}^2}$. Following arguments from the study of magnetic field effects in chemical reactions the characteristic field $B_{1/2}$ at which the spin effects reach the average of the value at zero field and at saturating field is correlated to the effective hyperfine fields in the radicals pair partners:[30]

$$B_{1/2} = 2\,\frac{(B_1^{hfc})^2 + (B_2^{hfc})^2}{(B_1^{hfc}) + (B_2^{hfc})} \qquad (16)$$

In our case, the value of $B_{1/2}$ calculated according to eq 16 is equal to 4.55 mT. Sometimes another estimate is used (cf. eq 155 in ref 31): $B_{1/2} = \sqrt{3}[(B_1^{hfc})^2 + (B_2^{hfc})^2]^{1/2}$ leading to $B_{1/2} = 5.26$ mT. Both values are in reasonable agreement with the experimental CIDNP data, $B_{1/2}^{exp} = 4.82 \pm 0.2$ mT, where the difference of the outer lines of the β-CH_2 quartet is taken as a measure of the multiplet effect.

Dynamic Effects. All our data are taken under conditions of quasi-continuous light irradiation and correspond to stationary CIDNP signals, which can be influenced by dynamic effects. Besides spin relaxation in the paramagnetic intermediate and in the diamagnetic end product the polarization kinetics may affect the signal amplitude. For cyclic processes, such as the reaction between histidine and dipyridyl, the same products are formed in the geminate recombination and in bulk reactions of radicals having escaped from geminate recombination. Accordingly, the stationary CIDNP signals have three contributions, namely:

(i) polarization from geminate recombination products;

(ii) polarization from radicals, which acquire spin order in geminate processes, escape geminate recombination, and recombine in bimolecular reactions in the bulk; and

(iii) polarization newly formed in the bulk, when radicals escaped from different geminate pairs meet in random collisions (F-pair polarization).

The field dependencies of the F-pair polarization and of the contribution from geminate recombination with triplet precursor are at high field described by the same eq 8, while the polarization of the escaped radicals depends on the mechanism of polarization. It has opposite sign with respect to the geminate product for the spin-sorting mechanism and the same sign for the spin-flipping channel. Hence, for cyclic reactions, bulk recombination tends to cancel nuclear polarization in the diamagnetic product at high magnetic field, while at low magnetic field no cancellation is expected. The resulting amplitude of stationary polarization is determined mainly by competition between the rate of radical recombination and the rate of nuclear spin−lattice relaxation in the radical state. Time-resolved measurements of CIDNP at a magnetic field of 7 T revealed rather short nuclear relaxation times of H-2 and H-4 protons in histidine radicals of 16 ± 5 μs,[15] corresponding to very efficient relaxation of nuclear polarization in radicals prior to their bulk recombination. In our experiment, laser irradiation of low power is used, and the estimated initial concentration of radicals, R_0, is about 1×10^{-5} M, much lower than in the

reported time-resolved experiments ($R_0 = 1.2 \times 10^{-4}$ M). We can therefore expect that in our experiments, having a slow bimolecular reaction between escaped radicals with rate $k_t = 2.0 \times 10^9$ M^{-1} s^{-1},[15] the efficient paramagnetic nuclear spin lattice relaxation of the H-2 and H-4 protons completely suppresses any contribution from escaped radicals to the formation of CIDNP. On the other hand, one can expect that the rate of spin lattice relaxation depends on the external magnetic field, and this dependence can, in principle, lead to a deviation of the experimental cw-CIDNP data from the calculated values. Since in the wide magnetic field range from 100 mT up to 7 T the agreement between the CIDNP simulation based on eq 8 and the experimental data is very good, two conclusions can be drawn: (i) assumption (7) is valid and (ii) any dependence of nuclear relaxation time on the external magnetic field has no observable effect on the CIDNP of the ring protons. For all polarized histidine protons the shape of the measured field dependence does not show any significant deviation from the calculated curve. Thus, it can be concluded that for paramagnetic nuclear relaxation caused by modulation of anisotropic magnetic interactions due to tumbling of histidine radicals with a correlation time τ_c the relation $\omega\tau_c \ll 1$ holds for the whole magnetic field range.

The field dependencies of net CIDNP for ring and β-CH_2 protons, when considered in the whole range from 0.1 mT to 7 T, not only differ by sign, but also by the ratio of CIDNP amplitude taken at high and at low field. For β-CH_2, the polarization at low field and at high field maximum has nearly the same amplitude, while for the ring protons CIDNP at the high-field maximum is about five times stronger than at the low-field counterpart. Keeping in mind that at low field the total electron and nuclear spin is conserved, and the electron singlet−triplet transitions are accompanied by nuclear spin flip, both the cage product and the escaped radical, are enriched in nuclear polarization of the same sign adding up in the diamagnetic reaction product. In this case, loss of polarization is more likely for the ring protons with their short relaxation, whereas at high field, where the spin-sorting mechanism of singlet−triplet transition ($S-T_0$) is operative, the described cancellation effect can reduce the stationary CIDNP amplitude more efficiently in case of the β-CH_2 protons due to their comparatively long spin−lattice relaxation time of 196 ± 25 μs.[15]

Conclusion

By using modern digital positioning techniques and working with a combination of current-controlled electromagnet and cryomagnet stray field it is possible to perform CIDNP measurements at variable field ranging from zero to several Tesla without sacrificing high spectral resolution. In this way, the formation of nuclear spin polarization can be precisely measured for individual nuclear positions in diamagnetic reaction products, and the relevant mechanisms of polarization can be determined. The scope of such an analysis is clear from our investigation of the photoinitiated intermolecular H-transfer reaction between histidine and dipyridyl. In this case, the high spectral resolution allowed us to observe and analyze in detail the CIDNP multiplet effect for the β-CH_2 protons and even for the imidazole ring protons with their spin−spin coupling below 2 Hz. From CIDNP nutation patterns the population selectivity of individual nuclear spin sublevels has been determined. The results unambiguously prove that the surprisingly efficient formation of nuclear polarization at fields below 5 mT is correlated with parallel orientation of scalar coupled nuclear spins.

Evaluation of multiplet and net effect as function of the magnetic field can provide information, which is not available from high field CIDNP experiments. In the present case, it is shown that exchange interaction does not play any major role in CIDNP formation. Numerical simulations of the net effect field dependence based on rather simple model assumptions reproduce the experimental data at fields above 0.1 T very well. This fact confirms also the validity of assuming a short lifetime of the geminate radical pairs in aqueous solution and reveals the limits of high field approximation. It opens the way to determine *g*-values and hyperfine coupling elements of short-lived reaction intermediates.

The experimental data obtained for the CIDNP field dependence of histidine are a good basis allowing to adjust the magnetic field strength for optimization of CIDNP detection of individual amino acid residues in proteins and in this way to increase the sensitivity and selectivity of the CIDNP method in application to protein structure analysis. The current trend in protein research by NMR is to go to higher and higher fields for the enhancement of sensitivity and resolution. That this approach is not always valid is demonstrated here: the very high efficiency of forming nuclear polarization with distinguishable pattern for histidine is found at a field of a few milli-Tesla. We think that in combination with detection at high field as presented in this contribution such polarization experiments will allow performing highly selective spin spectroscopy.

Acknowledgment. This work was supported by the DFG (Project No. Vi103/9), INTAS (Project No. 96-1269), and the Russian Foundation for Basic Research (Projects No. 99-03-33488 and 99-03-32753). A.V.Y. thanks the Alexander-von-Humboldt Foundation for a research fellowship at the Free University Berlin.

References and Notes

(1) Salikhov, K. M.; Molin, Yu. N.; Sagdeev, R. Z.; Buchachenko, A. L. *Spin Polarization and Magnetic Field Effects in Radical Reactions*; Elsevier: Amsterdam, 1984.

(2) Muus L. T.; Atkins P. W.; McLauchlan K. A.; Pedersen J. B. *Chemically Induced Magnetic Polarization*; Reidel: Dordrecht, 1977.

(3) Kaptein, R.; Dijkstra, K.; Nicolay, K. *Nature*, **1978**, *274*, 293−294.

(4) Kaptein, R. In *NMR Spectroscopy in Molecular Biology*; Pullman, B., Ed.; Reidel: Dordrecht, 1978; pp 211−229.

(5) Kaptein, R., In *Biological Magnetic Resonance, Vol.* 4; Berliner L. J., Reuben J., Eds.; Plenum Press: New York, 1982; pp 145−191.

(6) Hore, P. J.; Broadhurst, R. W. *Prog. NMR Spectrosc.* **1993**, *25*, 345−402.

(7) Hore, P. J.; Winder, S. L.; Roberts, C. H.; Dobson, C. M. *J. Am. Chem. Soc.* **1997**, *119*, 5049−5050.

(8) Broadhurst, R. W. D. Ph.D. Thesis, Oxford University, 1990.

(9) Winder, S. L. D. Ph.D. Thesis, Oxford University, 1997.

(10) Lyon, C. E. D. Ph.D. Thesis, Oxford University, 1999.

(11) Lopez, J. J.; Lyon, C. E.; Cho B. M.; Hore P. J. *Proceedings of the Joint 29th AMPERE-13th ISMAR International Conference*, Berlin, 1998; pp 462−463.

(12) Grosse, S.; Gubaydullin, F.; Scheelken, H.; Vieth, H.-M.; Yurkovskaya, A. V. *Appl. Magn. Reson.* **1999**, *17*, 211−225.

(13) Tsentalovich, Yu. P.; Morozova, O. B.; Yurkovskaya, A. V.; Hore, P. J. *J. Phys. Chem. A* **1999**, *103*, 5362−5368.

(14) Tsentalovich, Yu. P.; Morozova O. B. *J. Photochem. Photobiol., A: Chemistry* **2000**, *131*, 33−40.

(15) Tsentalovich, Yu. P.; Morozova, O. B.; Yurkovskaya, A. V.; Hore, P. J.; Sagdeev, R. Z.*J. Phys. Chem. A* **2000**, *104*, 6912−6916.

(16) Rao, P. S.; Sinic, M.; Hayon, E. *J. Phys. Chem.* **1975**, *79*, 1260−1263.

(17) Linnell, R. H.; Kaczmarczyk, A. *J. Phys. Chem.* **1961**, *65*, 1196−1199.

(18) Adrian F. J. *J. Chem. Phys.* **1971**, *54*, 3912−3917.

(19) Samuni, A.; Neta, P. *J. Phys. Chem.* **1973**, *77*, 1629−1635.

(20) Lassmann, G.; Erikson, L. A.; Himo, F.; Lendzian, F.; Lubitz, W. *J. Phys. Chem. A*, **1999**, *103*, 1283−1290.

(21) Wertz, J. G.; Bolton, J. R. *Electron Spin Resonance*, Chapman and Hall: New York, 1986.
(22) Gritsan, N. P., private communication, calculation using the program GAUSSIAN-94.
(23) Koenig, E.; Fischer, H. *Z. Naturforsch*. **1962**, *17a*, 1063.
(24) Landolt-Börnstein, *Magnetic Properties of Free Radicals*, Fischer, H.; Hellwege, K.-H., Eds.; Springer-Verlag: Berlin, 1977.
(25) Kaptein, R. *Chem. Commun*. **1971**, 732−733.
(26) Kaptein, R.; den Hollander, J. A. *J. Am. Chem. Soc.* **1972**, *94*, 6296.
(27) Fischer, H.; Lehnig M. *J. Phys. Chem.* **1971**, *75*, 3410.
(28) Schäublin, S.; Höhener, A.; Ernst, R. R. *J. Magn. Reson*. **1974**, *13*, 196−216.
(29) Ernst, R. R.; Bodenhausen, G.; Wokaun, A. *Principles of Nuclear Magnetic Resonance in One and Two Dimensions*, Clarendon Press: Oxford, 1987.
(30) Weller, A.; Nolting, F.; Staerk, H. *Chem. Phys. Lett.* **1983**, *97*, 24−27.
(31) Steiner, U. E.; Wolff, H.-J. in *Photochemistry and Photophysics, Vol. IV*, RCR Press: Boca Raton, 1994.